MHD MIXED CONVECTION SLIP FLOW NEAR A STAGNATION-POINT ON A NON-LINEARLY VERTICAL STRETCHING SHEET IN THE PRESENCE OF VISCOUS DISSIPATION

by

Stanford SHATEYI[a] and Fazle MABOOD[b*]

[a] Department of Mathematics, University of Venda, Thohoyandou, South Africa
[b] Department of Mathematics, University of Peshawar, Peshawar, Pakistan

Original scientific paper
https://doi.org/10.2298/TSCI151025219S

In this study, MHD mixed convection stagnation-point flow toward a non-linearly stretching vertical sheet in the presence of thermal radiation and viscous dissipation is numerically analyzed. The partial momentum and heat transfer equation are transformed into a set of ordinary differential equations by employing suitable similarity transformations. Using the Runge-Kutta Fehlberg fourth-fifth order method, numerical calculations to the desired level of accuracy are obtained for different values of dimensionless parameters. The results are presented graphically and in tabular form. The results for special cases are also compared to those obtained by other investigators and excellent agreements were observed. The effect of injection on the MHD mixed slip flow near a stagnation-point on a non-linearly vertical stretching sheet is to enhance the velocity field which results from the suppression of the skin friction on the wall surface. The heat transfer rate at the surface increases with increasing values of the non-linearity parameter. The velocity and thermal boundary-layer thicknesses are found to be decreasing with increasing values of the non-linearity parameter.

Key words: *MHD mixed convection, slip flow, non-linearly stretching sheet, thermal radiation, viscous dissipation*

Introduction

Much attention has been given to the stagnation-point flow due to stretching sheet because of its crucial practical applications. These applications include, extrusion of polymers, glass fiber, cooling of metallic plates, and aerodynamics. Stagnation flow is the name given to fluid flow near a stagnation-point. In the stagnation area, that is where fluid pressure and the rates of heat and mass transfer are highest. Hiemenz [1] pioneered the study of stagnation-point flow. Suali *et al.* [2] carried out analysis of the unsteady 2-D stagnation-point flow and heat transfer over a stretching/shrinking sheet with prescribed surface heat flux. Shateyi and Makinde [3] investigated stagnation-point flow and heat transfer of an electrically conducting incompressible viscous fluid with convective boundary conditions. Hayat *et al.* [4] analyzed the effects of mixed convection unsteady stagnation-point flow of a viscous fluid with a variable free stream velocity. There has been increasing interest in investigating the MHD with mixed convection boundary-layer flow and heat transfer over a stretching vertical surface. Ali *et al.* [5] analyzed the MHD mixed convection stagnation-point flow and heat transfer of an incompress-

* Corresponding author, e-mail: mabood1971@yahoo.com

ible viscous fluid over a vertical stretching sheet. Pal and Mondal [6] presented a numerical model to study the effects of temperature dependent viscosity and variable thermal conductivity on mixed convection problem.

Aman *et al.* [7] studied the steady 2-D stagnation-point flow over a linearly stretching/shrinking sheet in a viscous and incompressible fluid in the presence of a magnetic field. Sharma *et al.* [8] numerically studied the MHD stagnation-point flow of a viscous, incompressible and electrically conducting fluid over a stretching/shrinking permeable semi-infinite flat plate. Ishak *et al.* [9] investigated the steady 2-D MHD stagnation-point flow towards a stretching sheet with variable surface temperature. Hsiao [10] performed an analysis for heat and mass transfer of a steady laminar boundary-layer flow of an electrically magnetic conducting fluid of second-grade subject to suction and to a transverse uniform magnetic and electric field past a semi-infinite stretching sheet. Hsiao [11] studied MHD mixed convection heat transfer problem of a second-grade viscoelastic fluid past a wedge with porosity and suction or injection. Hsiao [12] investigated energy problems of conjugate conduction, convection and radiation heat, and mass transfer with viscous dissipation and magnetic effects.

The process of converting mechanical energy of downward flowing water into thermal and acoustical energy is known as viscous dissipation. Devices are designed in stream beds for example, to reduce the kinetic energy of flowing waters. This is meant to reduce their erosive potential on banks and river bottoms. Vajravelu and Hadjinicolaou [13] studied heat transfer characteristics over a stretching surface with viscous dissipation. More recently, Shen *et al.* [14] studied the problem of MHD mixed convection flow over a stagnation-point region over a non-linear stretching sheet with slip velocity and prescribed surface heat flux. Dessie and Kishan [15] analyzed MHD boundary-layer flow and heat transfer of a fluid with variable viscosity through a porous medium towards a stretching sheet by considering viscous dissipation. Jat and Chaudhary [16] investigated the problem of MHD boundary-layer flow over a stretching sheet for stagnation-point, heat transfer with and without viscous dissipation and Joule heating. Abel *et al.* [17] investigated numerically the problem of MHD flow and heat of an incompressible viscous fluid with the presence of buoyancy force and viscous dissipation. Ali [18] studied heat transfer and flow field characteristics of a stretched permeable surface subject to mixed convection.

The effects of thermal radiation are of vital importance in processes involving high temperatures and in space technology. Attention has recently being focused on the thermal radiation as a mode of energy transfer in hypersonic flights, missile re-entry, gas-cooled nuclear reactors, and rocket combustion chambers. Hossain *et al.* [19] studied the effect of thermal radiation on natural convectional flow of an optically thick viscous incompressible flow past a heated vertical porous plate. Shateyi and Motsa [20] investigated thermal radiation effects on heat and mass transfer over an unsteady stretching surface. Shateyi and Marewo [21] numerically analysed the problem of unsteady MHD flow near a stagnation-point of a 2-D porous body with heat and mass transfer in the presence of thermal radiation and chemical reaction. Shateyi [22] investigated thermal radiation and buoyancy effects on heat and mass transfer over a semi-infinite stretching surface with suction and blowing. Machireddy [23] studied the effects of Joule heating on steady MHD mixed convection boundary-layer flow over a stretched vertical flat plate in the presence of thermal radiation and viscous dissipation. Some related work with different geometries can be found in [24-32].

Andersson [33] in their study of the slip-flow of a Newtonian fluid past a linearly stretching sheet observed that the assumption of the convectional no-slip condition at the boundary is not always true and therefore should be replaced by partial slip boundary condi-

tions in certain situations. Chaudhary and Kumar [34] analyzed the steady 2-D MHD boundary-layer flow of a viscous, incompressible and electrically conducting fluid near a stagnation-point past a shrinking sheet with slip conditions. Abdel-Rahman [35] studied the problem of heat and mass transfer flow over a moving permeable flat stretching sheet in the presence of convective boundary condition, slip, radiation, heat generation/absorption, and first-order chemical reaction. Sharma *et al.* [36] investigated the boundary-layer flow and heat transfer over an exponentially shrinking sheet with slip effect. Mukhopadhyay [37] analyzed the effects of partial slip on boundary-layer over a non-linearly stretching surface with suction/injection.

Motivated by the previous studies, the current paper aims to numerically analyze the problem of MHD mixed slip flow near a stagnation-point on a non-linearly vertical stretching sheet in the presence of thermal radiation and viscous dissipation. The partial momentum and heat transfer equation are transformed into a set of ODE by employing suitable similarity transformations. Using the Runge-Kutta Fehlberg fourth-fifth order method, numerical calculations to the desired level of accuracy are obtained for different values of dimensionless parameters. The results are presented graphically and in tabular form. The results for special cases are also compared to those by Shen *et al.* [14], Wang [38], and Wong *et al.* [39]. Approximations of skin friction and the Nusselt number which are very crucial from engineering applications point of view are also presented in the present study. It is hoped that the results obtained in this study will serve as a complement to previous studies and also provide useful information for further studies.

Flow analysis and mathematical formulation

In this study we consider the steady 2-D MHD mixed convection flow near a stagnation-point over a non-linear stretching sheet with slip velocity, thermal radiation and viscous dispassion. We also consider a prescribed surface heat flux. We confine the flow to the region $y \geq 0$, where y is the co-ordinate measured perpendicular to the stretching surface. A uniform magnetic field of strength $B(x)$ is applied in the direction normal to the surface, fig. 1. The sheet stretching velocity is assumed to be $u_w(x) = cx^m$, and the external velocity is prescribed as $u_e(x) = ax^m$, where c and a are positive constants. While m is the non-linearity parameter, with $m = 1$ for the linear case and $m \neq 1$ for the non-linear case. Under the above assumptions and the boundary-layer and Boussinesq approximation, the governing equations for the current study are given by:

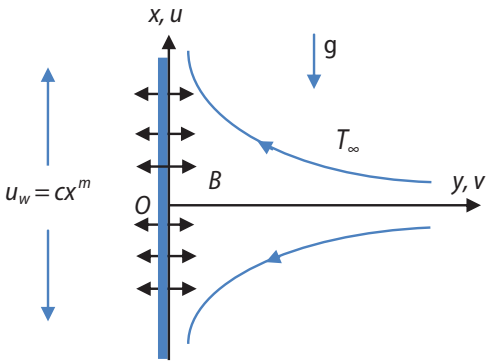

Figure 1. Physical model and co-ordinate system

$$\frac{\partial u}{\partial x} + \frac{\partial v}{\partial y} = 0 \tag{1}$$

$$u\frac{\partial u}{\partial x} + v\frac{\partial u}{\partial y} = u_e\frac{\mathrm{d}u_e}{\mathrm{d}x} + \nu\frac{\partial^2 u}{\partial y^2} - \frac{\sigma B^2(x)}{\rho}(u_e - u) + \mathrm{g}\beta(T - T_\infty) \tag{2}$$

$$u\frac{\partial T}{\partial x} + v\frac{\partial T}{\partial y} = \alpha\frac{\partial^2 T}{\partial y^2} + \frac{\mu}{\rho c_p}\left(\frac{\partial u}{\partial y}\right)^2 - \frac{1}{\rho c_p}\frac{\partial q_r}{\partial y} \tag{3}$$

where u and v are the velocity components in the x- and y-directions, respectively, ν – the kinematic viscosity, ρ – the fluid density, σ – the electrical conductivity, $B(x)$ – the transverse magnetic field, g – the acceleration due to gravity, β – the thermal expansion coefficient, T – the fluid temperature, α – the thermal diffusivity, c_p – the heat capacity at constant pressure, μ – the dynamic viscosity, and q_r – the radiative heat flux. The associated boundary conditions to the current model are given by:

$$y = 0: \quad u = u_w(x) + \frac{2-\delta_v}{\delta_v}\lambda_0 \frac{\partial u}{\partial y}, \quad v = v_w(x), \quad \frac{\partial T}{\partial y} = -\frac{q_w(x)}{k} \tag{4}$$

$$y \to \infty: \quad u \to u_e(x), \quad T \to T_\infty \tag{5}$$

where δ_v is the tangential momentum accommodation coefficient, λ_0 – the mean free path, $v_w(x)$ – the suction injection velocity, k – the thermal conductivity, and q_w – the surface heat flux. By using the Rosseland diffusion approximation, Hossain *et al.* [40], Raptis [41], among other researchers, the radiative heat flux, q_r, is given by:

$$q_r = \frac{-4\sigma^* T_\infty^{\,3}}{3K_s}\frac{\partial T^4}{\partial y} \tag{6}$$

where σ^* and K_s are the Stefan-Boltzman constant and the Rosseland mean absorption coefficient, respectively. We assume that the temperature differences within the flow are sufficiently small so that T^4 may be expressed as a linear function of temperature, T.

$$T^4 \approx 4T_\infty^{\,3}T - 3T_\infty^{\,4} \tag{7}$$

Using eqs. (9) and (10) in the fifth term of eq. (3) we obtain:

$$\frac{\partial q_r}{\partial y} = \frac{-16\sigma^* T_\infty^{\,3}}{3K_s}\frac{\partial^2 T}{\partial y^2} \tag{8}$$

Similarity analysis

Following Shen *et al.* [14] we introduce the following similarity transformations:

$$\eta = \sqrt{\frac{a}{\nu}}\, y x^{\frac{m-1}{2}}, \quad \psi = \sqrt{a\nu}\, x^{\frac{m+1}{2}} f(\eta), \quad \theta = \sqrt{\frac{a}{\nu}}\,\frac{k(T-T_\infty)}{q_0 x^{2m-1}} \tag{9}$$

Here ψ is the stream function such that $u = \partial\psi/\partial y$, $v = -\partial\psi/\partial x$ and continuity equation is automatically satisfied. By suing eq. (9), the velocity components for u and v are given:

$$u = ax^m f'(\eta), \quad v = -\sqrt{a\nu}\, x^{(m-1)/2}\left[\frac{m+1}{2} f(\eta) + \frac{m-1}{2}\eta f'(\eta)\right] \tag{10}$$

where primes denote differentiation with respect to η.

We remark that to obtain similarity solutions, $B(x)$, $v_w(x)$, and $q_w(x)$ are taken:

$$B(x) = B_0 x^{\frac{m-1}{2}}, \quad v_w = -\frac{\sqrt{a\nu}\,(m+1)}{2} x^{\frac{m-1}{2}} f_w, \quad q_w(x) = q_0 x^{\frac{5m-3}{2}} \tag{11}$$

where B_0, f_w, and q_0 are arbitrary constants. We also have $f_w > 0$ corresponding to the injection case and $f_w < 0$ implying suction. Upon substituting the similarity variables into eqs. (2) and (3), we obtain the following system of ODE:

$$f''' + \left(\frac{m+1}{2}\right) ff'' + m\left(1 - f'^2\right) - M\left(f' - 1\right) + \lambda\theta = 0 \tag{12}$$

$$\left(\frac{4+3R}{3\,\mathrm{Pr}\,R}\right)\theta'' + \left(\frac{m+1}{2}\right) f\theta' - \left(2m-1\right) f'\theta + \mathrm{Ec} f''^2 = 0 \tag{13}$$

The corresponding boundary conditions to the transformed equations are:

$$f(0) = f_w,\ f'(0) = \varepsilon + \delta f''(0),\ \theta'(0) = -1 \tag{14}$$

$$f'(\infty) = 1,\ \theta(\infty) = 0 \tag{15}$$

We have $M = B_0^2/\rho a$ is the magnetic parameter, $\lambda = \mathrm{g}\beta q_0 (\nu)^{1/2}/ka^{5/2}$ is the mixed convection parameter, Pr = ν/α is the Prandtl number, $R = 4\sigma^* T^3/\rho c_p k_1$ is the thermal radiation parameter, Ec = $a^{5/2}x^{3m}/\rho c_p$ is the Eckert number, (as the Eckert number depends on x, the solutions obtained are local similarity solutions), $\varepsilon = c/a$ is the velocity ratio parameter, $\delta = \left(2 - \sigma_v\right) k x_n \,\mathrm{Re}_x^{1/2}/\sigma_v$ is the velocity slip parameter. The quantities of engineering interest in this study are the skin friction coefficient, C_f, and the Nusselt number, Nu_x, which are defined:

$$C_f = \frac{\tau_w(x)}{\rho u_p^2}, \quad \mathrm{Nu}_x = \frac{x q_w(x)}{k(T_w - T_\infty)} \tag{16}$$

with the surface shear stress $\tau_w(x) = \partial u/\partial y|_{y=0}$ and $q_w(x)$ is the wall heat flux. We then obtain the following expressions after applying the similarity variables:

$$\mathrm{Re}_x^{1/2} C_f = f''(0), \quad \mathrm{Re}_x^{-1/2} \mathrm{Nu}_x = \frac{1}{\theta(0)} \tag{17}$$

with $\mathrm{Re}_x = u_e x/\nu$ being the Reynolds number.

Method of solution

In this study, an efficient numerical scheme Runge-Kutta Fehlberg fourth-fifth order method has been employed to investigate the flow model defined by eqs. (12) and (13) with the boundary eqs. (14) and (15) for different values of controlling parameters. The formula for the Runge-Kutta-Fehlberg fourth fifth order numerical method is given:

$$k_0 = f\left(x_i,\, y_i\right)$$

$$k_1 = f\left(x_i + \frac{1}{4}h,\, y_i + \frac{1}{4}hk_0\right)$$

$$k_2 = f\left[x_i + \frac{3}{8}h,\, y_i + \left(\frac{3}{32}k_0 + \frac{9}{32}k_1\right)h\right] \tag{18}$$

$$k_3 = f\left[x_i + \frac{12}{13}h,\, y_i + \left(\frac{1932}{2197}k_0 - \frac{7200}{2197}k_1 + \frac{7296}{2197}k_2\right)h\right]$$

$$k_4 = f\left[x_i + h,\, y_i + \left(\frac{439}{216}k_0 - 8k_1 + \frac{3860}{513}k_2 - \frac{845}{4104}k_3\right)h\right]$$

$$k_5 = f\left[x_i + \frac{1}{2}h,\ y_i + \left(-\frac{8}{27}k_0 + 2k_1 - \frac{3544}{2565}k_2 + \frac{1859}{4104}k_3 - \frac{11}{40}k_4\right)h\right]$$

$$y_{i+1} = y_i + \left(\frac{25}{216}k_0 + \frac{1408}{2565}k_2 + \frac{2197}{4104}k_3 - \frac{1}{5}k_4\right)h \tag{18}$$

$$z_{i+1} = z_i + \left(\frac{16}{135}k_0 + \frac{6656}{12825}k_2 + \frac{28561}{56430}k_3 - \frac{9}{50}k_4 + \frac{2}{55}k_5\right)h$$

where y is the fourth-order Runge-Kutta and z is the fifth-order Runge-Kutta. An estimate of the error can be obtained by subtracting the two values obtained. If the error exceeds a specific threshold, the results can be re-calculated using a smaller step size. The approach to estimating the new step size is:

$$h_{\text{new}} = h_{\text{old}} \sqrt[4]{\frac{\varepsilon h_{\text{old}}}{2\left|z_{i+1} - y_{i+1}\right|}} \tag{19}$$

Computations were carried out with $\Delta\eta = 0.01$. The requirement that the variation of the dimensionless velocity and temperature is less than 10^{-6} between any two successive iterations is employed as the criterion convergence. The asymptotic boundary conditions in eq. (15) were approximated by using a value of 10 for $\eta_{\max}$:

$$\eta_{\max} = 10, \quad f'(10) = 1,\ \theta(10) = 0 \tag{20}$$

This ensures that all numerical solutions approached the asymptotic values correctly.

The effects of the emerging parameters on the dimensionless velocity, temperature, skin friction coefficient, and the rate of heat transfer are investigated. To validate the present solution, comparison has been made with previously published data from the literature for skin friction coefficient and heat transfer rate in tab. 1. In tab. 2 we have provided comparison of $f''(0)$ values with other published results and they are found to be in a favorable agreement. Table 3 presents the effects of various parameters on skin friction coefficient and heat transfer rate. It is clearly seen that with R and Eckert number heat transfer rate is decreasing whereas it is increasing with f_w and m.

Table 1. Comparison of skin friction coefficient and Nusselt number for different values of ε

ε	HAM in [14]		Present	
	$f''(0)$	$1/\theta(0)$	$f''(0)$	$1/\theta(0)$
0.1	0.6599	2.1772	0.659878	2.176819
1	–0.0248	2.2670	–0.024792	2.266589
2	–0.7945	2.3593	–0.794489	2.358832

Table 2. Comparison of the values of $f''(0)$ with those of Wang [38] and Wong *et al.* [39] when $f_w = \delta = \lambda = M = 0$, $m = 1$

ε	Wang [38]	Wong *et al.* [39]	Present results
0	1.232588	1.23259	1.232587
0.1	1.14656	1.14656	1.146561
0.2	1.05113	1.05113	1.051129
0.5	0.71330	0.71329	0.713295
1	0	0	0
2	−1.88731	−1.88730	–1.887307
5	−10.26475	−10.26475	–10.264749

Results and discussion

In this section, a comprehensive numerical parametric study is contacted and the results are presented in tabular and graphical forms. Stretching greatly reduces the skin friction on the wall surface but increases the rate of heat transfer as can be clearly seen in tab. 1. Fluid injection leads to the reduction of the skin friction as can be observed in

tab. 3. However, the rate of heat transfer increases as the values of injection parameter increase. Increasing the non-linearity parameter, m, has very insignificant effect on the skin friction as well as on the Nusselt number. In tab. 3, we also observe that the thermal radiation parameter increases the values of the skin friction but greatly reduces the values of the Nusselt number.

Table 3. Values of skin friction coefficient and Nusselt number for different values of $\delta = \lambda = M = \mathrm{Pr} = 1$

f_w	m	λ	R	Ec	$f''(0)$	$1/\theta(0)$
0	1	1	1	1	0.14286	0.87121
0.5					0.11852	0.98907
1					0.097006	1.11964
	1.5				0.057518	1.42527
	2				0.038958	1.68721
	3				0.021821	2.14261
	1	–0.5			–0.05357	1.06907
		0			0	1.08848
		0.5			0.049915	1.10516
		1	2		0.142057	0.85849
			3		0.180387	0.72148
			5		0.243881	0.57346
			1	2	0.097256	1.11780
				5	0.098017	1.11222
				10	0.099332	1.10272

Graphical representations of the numerical results are illustrated in figs. 2-11. Figures 2(a) and 2(b) depicts the influence of suction/injection parameter, f_w, on the velocity profiles for both assisting and opposing cases. It can be seen that increasing the mixed buoyancy parameter causes the velocity profiles to increase. We can also observe that the velocity profiles are significantly influenced by suction/injection parameter, f_w. The velocity boundary-layer is greatly enhanced by the injection parameter. Injecting fluid into the flow system causes the velocity to increase as expected. This shows that injection can accelerate the fluid flow transition from laminar to turbulent. It is observed also in this figure that removing the fluid through suction from the flow system reduces the velocity profiles.

In fig. 3(a), we depict the influence of the slip velocity in both assisting and opposing cases. The velocity profiles are reduced by increasing the values of the slip velocity in the opposing or cooling flow. In the assisting case, we see that increasing the values of the slip velocity leads to increasing values of the velocity profiles near the stretching sheet surface. The velocity increases to a peak and gradually dies down for a slip velocity value. The significant influence of the slip velocity on the flow properties substantiate the notion that the slip conditions can not be neglected in some cases. In fig. 3(b) we display the influence of the non-linearity parameter

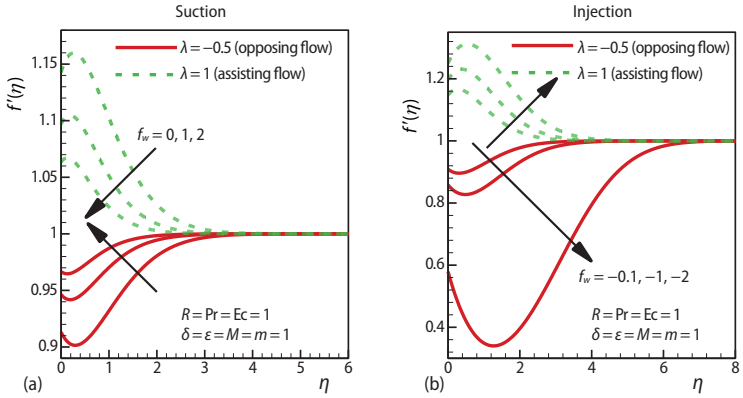

Figure 2. Effects of suction/injection and mixed convection parameters on dimensionless velocity

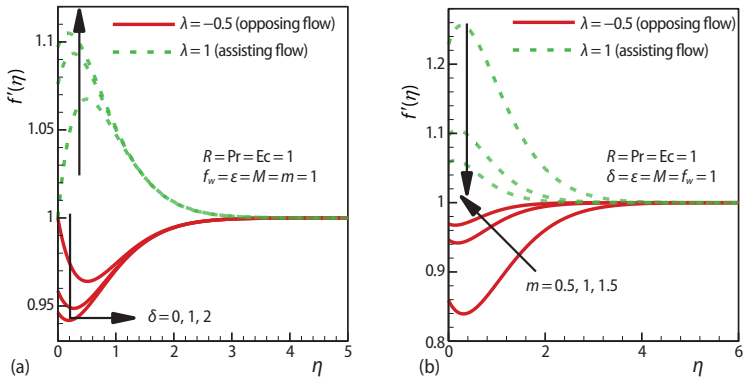

Figure 3. Effects of velocity slip, mixed convection, and non-linearity parameters on dimensionless velocity

in both opposing and assisting flow cases. In opposing flow case we observe that the velocity profiles are greatly increased when the values of the non-linearity parameter are increased. As the fluid temperature is reduced by cooling ($\lambda < 0$), the non-linearity of the sheet helps to destabilize the fluid flow thereby increases the velocity flow. This explains why we have reduced velocity values. However, an opposite effect of increasing values of the non-linearity parameter on the velocity profiles in the case of assisting flow is experienced. Buoyancy effect as a driving force for fluid flow increases the velocity profiles but as the non-linearity parameter increases, we observe that the profile increase to peak and then dies to the free stream velocity.

In fig. 4(a), we have the influence of the Prandtl number on the velocity profiles. As the Prandtl number is the ratio of the momentum diffusivity to thermal diffusivity, increasing the values of the Prandtl number means that the momentum diffusivity is more significant than thermal diffusivity. This in turn causes the velocity profiles to greatly increase as can be clearly seen in fig. 4(a) for the assisting case. However, opposite effects are experienced for opposing flow case.

In fig. 4(b), we display the effect of the velocity ratio parameter on the velocity profiles. Increasing the values of the velocity ratio parameter physically means that the stretching velocity is much more than the external velocity. This in turn accelerates the fluid velocity as can be clearly seen in fig. 4(b).

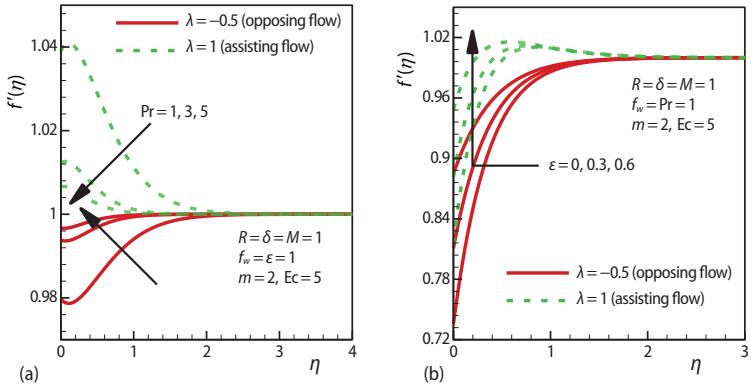

Figure 4. Variation of the velocity ratio, Prandtl number, and mixed convection on the velocity profiles

In fig. 5(a), we depict the influence of the thermal radiation on the velocity profiles. Increasing the values of the thermal radiation parameter increases the fluid velocity. Physically, increasing the values of the thermal radiation corresponds to an increased dominance of conduction over absorption radiation thereby increasing buoyancy force and in turn increases the velocity profiles. Figure 5(b) displays the influence of the Eckert number on the velocity profiles. Increasing the values of the Eckert number allows energy to be stored in the fluid region as a result of dissipation due to viscosity and elastic deformation thus generating heat due to frictional heating. This then causes the velocity to be greatly increased.

Figures 6(a) and 6(b) shows the effects of suction and injection on the temperature profiles. Removing fluid from the flow system causes reduction of the thermal boundary-layer thickness while injecting fluid into the flow system causes enhancement of the thermal boundary-layer thickness. Therefore, suction reduces the thermal boundary-layer thickness. On the other, injection causes the temperature of the fluid to greatly increase.

The effects of varying the slip velocity and the velocity ratio parameters, are displayed in figs. 7(a) and 7(b), respectively. Increasing the slip velocity leads to the thinning of the thermal boundary-layer. As the slip velocity increases, the fluid flow get more accelerated thereby

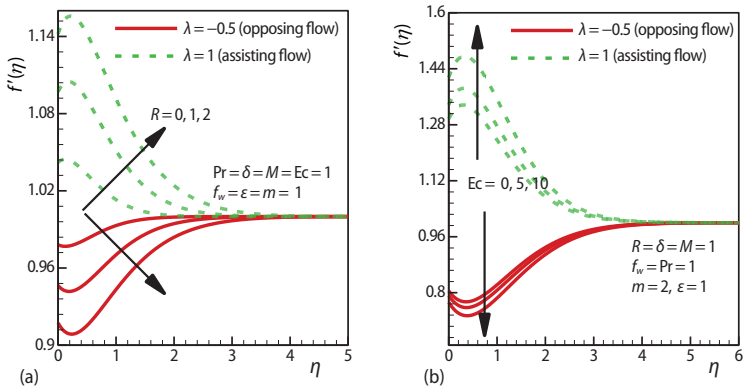

Figure 5. Variation of the thermal radiation parameter and Eckert number on dimensionless velocity

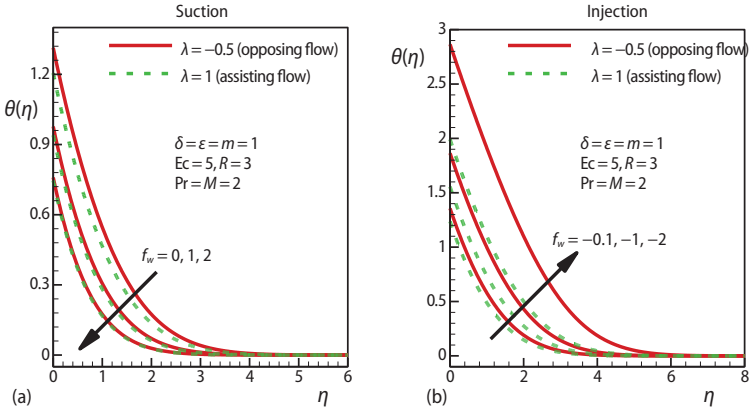

Figure 6. Effects of suction/injection and mixed convection parameters on dimensionless temperature profiles

driving the hot fluid downstream thus reducing the fluid temperature. In fig. 7(b), we observe that increasing the velocity ratio parameter causes the fluid temperature to increase.

The effect on non-linearity parameter on the temperature is depicted in fig. 8(a). We observe that the wall temperature decreases with increasing values of m. Increasing the velocity ratio parameter means that the stretching sheet velocity is being increased thereby accelerating the fluid flow thus reducing the fluid temperature. The influence of the thermal radiation on the fluid temperature is depicted in fig. 8(b). Divergence of the radiative heat flux increases as the Rosseland radiative absorption, k_1, decreases, which in turn increases the rate of radiative heat to the fluid. This then causes the thermal temperature boundary-layer to increase.

Figure 9(a) depicts the influence of the Eckert number on the fluid temperature. Increasing the Eckert number causes the storage of energy in the fluid region as a result of dissipation which is caused by viscosity and elastic deformation thus generating heat due to frictional heating. Thus great viscous dissipative heat causes significant rises in the fluid temperature. In fig. 9(b), the influence of Prandtl number on the fluid temperature is depicted. We notice that increasing the values of the Prandtl number results in reducing the thermal boundary-layer thick-

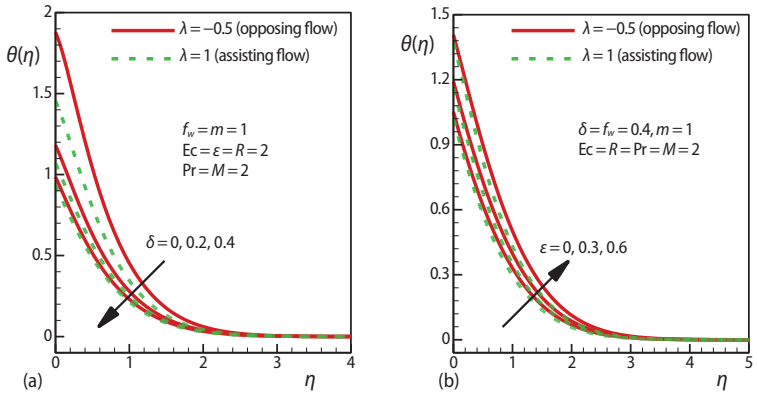

Figure 7. Effects of velocity slip, mixed convection, and velocity ratio parameters on dimensionless temperature

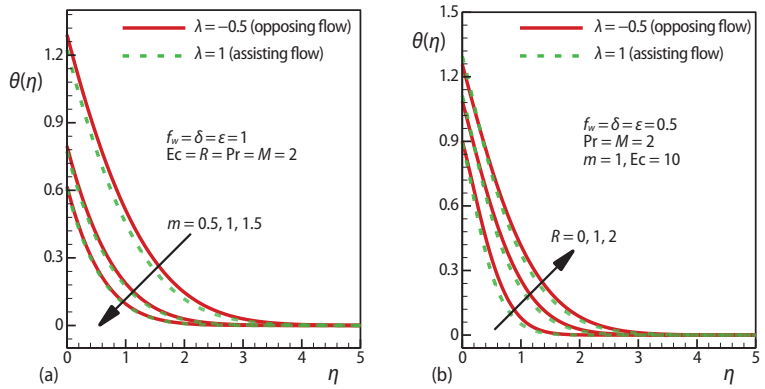

Figure 8. Variation of the non-linearity parameter, thermal radiation parameter, and mixed convection parameter on dimensionless temperature profiles

ness and then effectively lower the average temperature within the boundary-layer. Physically, smaller values of the Prandtl number, are equivalent to increasing the thermal conductivities, and therefore more heat can easily diffuse away from the heated stretching surface than for higher values of the Prandtl number.

Figure 10(a) shows the effect of varying the magnetic strength parameter on the skin friction coefficient in both opposing and assisting flow cases. As expected, the skin friction increases as the magnetic field strength values increase. Physically, the application of a magnetic field perpendicular to the fluid flow produces a drag force which tends to retard the fluid flow velocity, thus increasing the skin friction coefficient. In fig. 10(b), we display the effect of the velocity ratio parameter on the skin friction coefficient. As expected, increasing the stretching sheet velocity has significant effect on the skin friction coefficient. The skin friction is greatly reduced when the values of the stretching velocity of the sheet are increased.

The influence of the magnetic field strength on the rate of heat transfer is depicted in fig. 11(a). We clearly observe that the Nusselt number is reduced as the values of the magnetic parameter are increased. The influence of the thermal radiation parameter on the rate of heat transfer is depicted in fig. 11(b). As expected, the rate of heat transfer is greatly reduced by

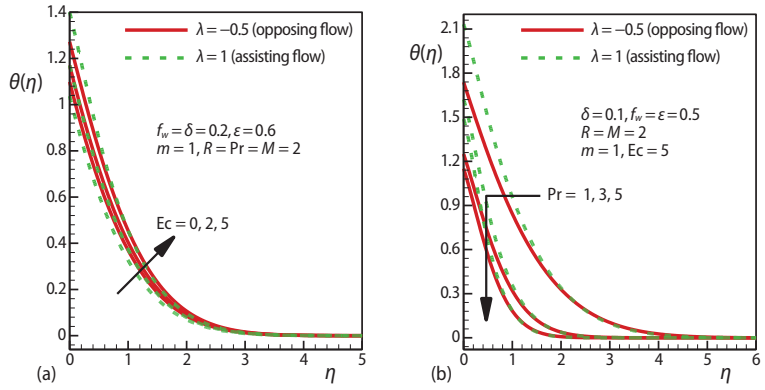

Figure 9. Effects of Eckert number, mixed convection and Prandtl number on dimensionless temperature

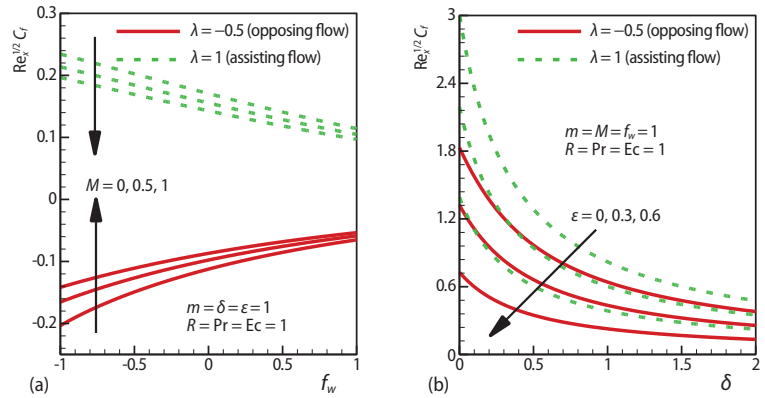

Figure 10. Variation of skin friction coefficient with velocity ratio, magnetic field, and mixed convection parameter

increasing values of the thermal radiation but increases as the values of the Prandtl number are increased. Finally, in figs. 12(a) and 12(b), we illustrate the effects of radiation and Eckert number on skin friction coefficient and Nusselt number. It is seen from fig. 12(a) that the skin friction coefficient is an increasing function of both R and Eckert number, while in fig. 12(b) the opposite effects of both R and Eckert number Nusselt number are observed.

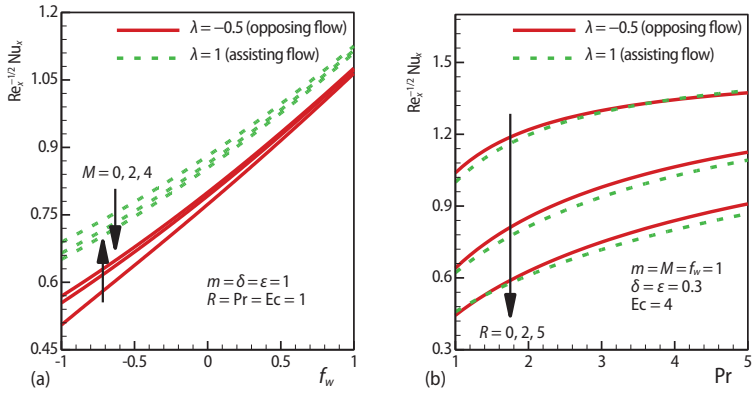

Figure 11. Variation of heat transfer rate with radiation, magnetic field, and suction/injection slip parameters, and Prandtl number

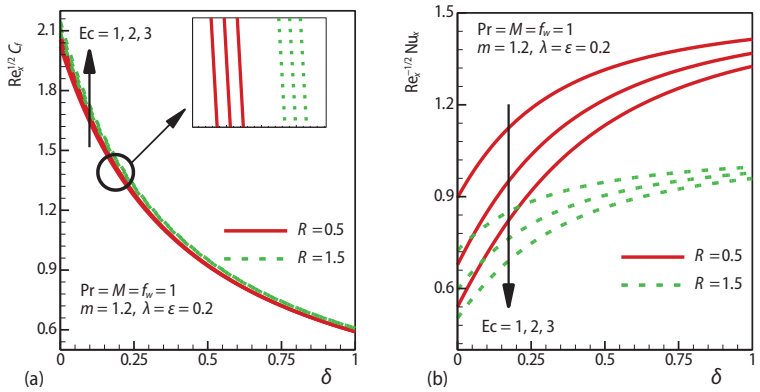

Figure 12. Variation of skin friction coefficient and heat transfer rate with radiation velocity ratio, and dissipation parameters

Conclusions

In this study, MHD mixed convection stagnation-point flow toward a non-linearity stretching vertical sheet in the presence of thermal radiation and viscous dissipation is numerically analyzed. The numerical solutions for momentum and energy equations have been obtained by the Runge-Kutta Fehlberg method. Based on the present study, the following conclusions are made.

- The velocity field is suppressed by increasing values of the suction parameter. This in turn enhances the skin friction coefficient.
- The effect of injection on the MHD mixed slip flow near a stagnation-point on a non-linearly vertical stretching sheet is to enhance the velocity field which results from the suppression of the skin friction on the wall surface.

- The heat transfer rate at the surface increases with increasing values of the non-linearity parameter, *m*. The velocity and thermal boundary-layer thicknesses are found to be decreasing with increasing values of the non-linearity parameter.
- The velocity increases with increasing values of the magnetic field parameter, velocity ratio parameter, thermal radiation, and Eckert number but decreases with increasing values of the thermal radiation and slip velocity parameter.

In some cases, different flow behaviors were observed with opposing and assisting flows under different parameters.

Acknowledgment

The authors would like to thank the anonymous reviewers for their comments and suggestions which led to the improvement of this paper.

Nomenclature

a, c, q_0 – constants, [–]
$B(x)$ – strength of the imposed magnetic field, [Am^{-1}]
B_0 – arbitrary constant
c_p – specific heat capacity, [$Jkg^{-1}K^{-1}$]
C_f – skin friction coefficient
Ec – Eckert number, [–]
f – dimensionless stream function, [–]
f_w – suction/injection parameter, [ms^{-1}]
f' – dimensionless velocity, [–]
g – acceleration due to gravity, [ms^{-2}]
h – step size, [m]
K_s – mean absorption coefficient
k – thermal conductivity of the fluid, [$Wm^{-1}K^{-1}$]
M – magnetic parameter
m – the non-linearity parameter
Pr – Prandtl number, [–]
q_r – radiative heat flux, [Wm^{-2}]
R – radiation parameter
Re_x – local Reynolds number, [–]
T – fluid temperature, [K]
T_w – surface temperature, [K]
T_∞ – ambient temperature, [K]
u, v – velocity components along the x-, y-directions, respectively, [ms^{-1}]
$u_e(x)$ – external velocity, [ms^{-1}]
$u_w(x)$ – stretching sheet velocity, [ms^{-1}]
$v(w)$ – suction/injection velocity, [ms^{-1}]
x, y – Cartesian co-ordinates along the stretching surface normal to it, [m]

Greek symbols

α – thermal diffusivity, [m^2s^{-1}]
β – thermal expansion coefficient, [K^{-1}]
δ – slip velocity parameter, [ms^{-1}]
ε – velocity ratio parameter, [–]
θ – dimensionless temperature, [–]
λ – constant buoyancy parameter
λ_0 – the mean free path
μ – dynamic viscosity, [$kgm^{-1}s^{-1}$]
ν – kinematic viscosity, [m^2s^{-1}]
ρ – fluid density, [kgm^{-3}]
σ – the electrical conductivity, [Ωm]
σ_v – tangential momentum components
σ^* – Stefan-Boltzmann constant
τ_w – wall shear stress, [Pa]
ψ – stream function, [$kgm^{-1}s^{-1}$]

References

[1] Hiemenz, K. K., Die Grenzschicht an einem in den gleichformingen Flussigkeitsstrom eingetauchten graden Kreiszylinder, *Dinglers Polytechnic J., 326* (1911), pp. 321-324
[2] Suali, M., *et al.,* Unsteady Stagnation Point Flow and Heat Transfer over a Stretching/Shrinking Sheet with Prescribed Surface Heat Flux, *App. Math. Comp. Int., 1* (2012), July, pp. 1-11
[3] Shateyi, S., Makinde, O. D., Hydromagnetic Stagnation-Point Flow Towards a Radially Stretching Convectively Heated Disk, *Math. Prob. Eng.*, *2013* (2013), ID 616947
[4] Hayat, T., *et al.*, MHD Flow and Heat Transfer over Permeable Stretching Sheet with Slip Conditions, *Int. J. Numer. Meth. Fluids*, *66* (2011), 8, pp. 963-975
[5] Ali, F. M., *et al.,* Mixed Convection Stagnation-Point Flow on Vertical Stretching Sheet with External Magnetic Field, *Appl. Math. Mech.*, *35* (2014), 2, pp. 155-166
[6] Pal, D., Mondal, H., Effects of Temperature-Dependent Viscosity and Variable Thermal Conductivity on MHD Non-Darcy Mixed Convective Diffusion of Species over a Stretching Sheet, *J. Egyptian Math. Soc., 22* (2014), 1, pp. 123-133

[7] Aman, F., *et al.,* Magnetohydrodynamic Stagnation-Point Flow Towards a Stretching/Shrinking Sheet with Slip Effects, *Int. Commun. Heat . Mass Transf., 47* (2014), Oct., pp. 6872
[8] Sharma, R., *et al.,* Stability Analysis of Magnetohydrodynamic Stagnation Point Flow Toward a Stretching/Shrinking Sheet, *Computers & Fluids, 102* (2014), Oct., pp. 9498
[9] Ishak, A., *et al.*, MHD Stagnation Point Flow Towards a Stretching Sheet, *Physica A*, *388* (2009), 17, pp. 3377-3383
[10] Hsiao, K. L., Heat and Mass Mixed Convection for MHD Visco-Elastic Fluid Past a Stretching Sheet with Ohmic Dissipation, *Commun. Nonlinear Sci. Numer. Simul*., *15* (2010), 7, pp. 1803-1812
[11] Hsiao, K. L., MHD Mixed Convection for Viscoelastic Fluid Past a Porous Wedge, *Int. J. Non-Linear Mech., 46* (2011), 1, pp. 1-8
[12] Hsiao, K. L., Nanofluid Flow with Multimedia Physical Features for Conjugate Mixed Convection and Radiation, *Computers & Fluids, 104* (2014), Nov., pp. 1-8
[13] Vajravelu, K., Hadjinicolaou, A., Heat Transfer in a Viscous Fluid over a Stretching Sheet with Viscous Dissipation and Internal Heat Generation, *Int. Comm. Heat Mass Transf., 20* (1993), 3, pp. 417-430
[14] Shen, M., *et al.,* MHD Mixed Convection Slip Flow Near a Stagnation Point on a Nonlinearly Vertical Stretching Sheet, *Boundary Value Prob., 2015* (2015), Dec., pp. 78-92
[15] Dessie, H., Kishan, K., MHD Effects on Heat Transfer over Stretching Sheet Embedded in Porous Medium with Variable Viscosity, Viscous Dissipation and Heat Source/Sink, *Ain Shains Eng. J., 5* (2014), 3, pp. 967-977
[16] Jat, R. N., Chaudhary, S., Magnetohydrodynamic Boundary Layer Flow Near the Stagnation Point of a Stretching Sheet, *Il Nuovo Cimento*, *123* (2008), B, pp. 555-566
[17] Abel, M. S., *et al.,* MHD Flow, and Heat Transfer with Effects of Buoyancy, Viscous and Joules Dissipation over a Nonlinear Vertical Stretching Porous Sheet with Partial Slip, *Engineering*, *3* (2011), 3, pp. 285-291
[18] Ali, M., Mixed Convection Boundary Layer Flows Induced by a Permeable Continuous Surface Stretched with Prescribed Skin Friction, *World Academy of Science, Eng. Tech., 7* (2013), 6, pp. 633-637
[19] Hossain, M. A., *et al.,* The Effect of Radiation on Free Convection from a Porous Vertical Plate, *Int. J.Heat Mass Transf., 42* (1999), 1, pp. 181-191
[20] Shateyi, S., Motsa, S. S., Thermal Radiation Effects on Heat and Mass Transfer over an Unsteady Stretching Surface, *Math.* P*rob. Eng., 2009* (2009), ID 965603
[21] Shateyi, S., Marewo, G. T., Numerical Analysis of Unsteady MHD Flow Near a Stagnation-Point of a Two Dimensional Porous Body with Heat and Mass Transfer, Thermal Radiation and Chemical Reaction, *Boundary Value Prob., 2014* (2014), Dec., pp. 218-235
[22] Shateyi, S., Thermal Radiation and Buoyancy Effects on Heat and Mass Transfer over a Semi-Infinite Stretching Surface with Suction and Blowing, *J. Appl. Math., 2008* (2008), ID 414830
[23] Machireddy, G. R., Influence of Thermal Radiation, Viscous Dissipation and Hall Current on MHD Convection Flow over a Stretched Vertical Flat Plate, *Ain Shams Eng. J., 5* (2014), 1, pp. 169-175
[24] Ferdows, M., *et al.,* MHD Mixed Convective Boundary Layer Flow of a Nanofluid through a Porous Medium Due to an Exponentially Stretching Sheet, *Math. Prob. Eng.*, *2012* (2012), ID 408528
[25] Ferdows, M., *et al.,* Numerical Study of Transient Magnetohydrodynamic Radiative Free Convection Nanofluid Flow from a Stretching Permeable Surface, *J. Process Mech. Eng., 228* (2014), 3, pp. 1-16
[26] Beg, O. A., *et al.,* Explicit Numerical Study of Unsteady Hydromagnetic Mixed Convective Nanofluid Flow from an Exponential Stretching Sheet in Porous Media, *Appl. Nanosci., 4* (2013), 8, pp. 943-957
[27] Wahiduzzaman, W., *et al.,* Viscous Dissipation and Radiation Effects on MHD Boundary Layer Flow of a Nanofluid Past a Rotating Stretching Sheet, *Appl. Math., 6* (2015), 3, pp. 547-567
[28] Wahiduzzaman, W., *et al.,* MHD Convective Stagnation Flow of Nanofluid over a Shrinking Surface with Thermal Radiation, Heat Generation and Chemical Reaction, *Proce. Eng., 105* (2015), Dec., pp. 398-405
[29] Shakhaoath, Md. K., *et al.,* MHD Boundary Layer Radiative, Heat Generating and Chemical Reacting Flow Past a Wedge Moving in a Nanofluid, *Nano Converg., 1* (2014), 1, pp. 1-13
[30] Shakhaoath, Md., *et al*., Effects of Magnetic Field on Radiative Flow of a Nanofluid Past a Stretching Sheet, *Proce. Eng., 56* (2013), May, pp. 316-322
[31] Dinarvand, S., *et al.,* Homotopy Analysis Method for Mixed Convection Boundary-Layer Flow of a Nanofluid over a Vertical Circular Cylinder, *Thermal Science, 19* (2015), 2, pp. 549-561
[32] Rashidi, M. M., *et al.,* Mixed Convection Boundary-Layer Flow of a Micro Polar Fluid Towards a Heated Shrinking Sheet by Homotopy Analysis Method, *Thermal Science, 20* (2016), 1, pp. 21-34
[33] Andersson, H. I., Slip Flow Past a Stretching Surface, *Acta Mechanica, 158* (2002), 1-2, pp. 121-125

[34] Chaudhary, S., Kumar, P., MHD Slip Flow past a Shrinking Sheet, *Appl. Math., 4* (2013), 3, pp. 574-581
[35] Abdel-Rahman, R. G., MHD Slip Flow of Newtonian Fluid Past a Stretching Sheet with Thermal Convective Boundary Condition, Radiation, and Chemical Reaction, *Math. Prob. Eng., 2013* (2013), ID 359817
[36] Sharma, R., *et al.,* Boundary Layer Flow and Heat Transfer over a Permeable Exponentially Shrinking Sheet in the Presence of Thermal Radiation and Partial Slip, *J. Appl.Fluid Mech., 7* (2014), 1, pp. 125-134
[37] Mukhopadhyay, S., Analysis of Boundary Layer Flow over a Porous Nonlinearly Stretching Sheet with Partial Slip at the Boundary, *Alexandria Eng. J., 52* (2013), 4, pp. 563-569
[38] Wang, C. Y., Stagnation Flow Towards a Shrinking Sheet, *Int. J. NonLinear Mech., 43* (2008), 5, pp. 377-382
[39] Wong, S. W., *et al.,* Stagnation-Point Flow Toward a Vertical, Nonlinearly Stretching Sheet with Prescribed Surface Heat Flux, *J. Appl. Math., 2013* (2013), ID 528717
[40] Hossain, M. A. *et al.,* The Effect of Radiation on Free Convection Flow of Fluid with Variable Viscosity from a Vertical Porous Plate, *Int. J. Therm. Sci., 40* (2001), 2, pp. 115-124
[41] Raptis, A., Flow of a Micropolar Fluid Past a Continuously Moving Plate by the Presence of Radiation, *Int. J. Heat Mass Transf., 41* (1998), 18, pp. 2865-2866
[42] Faires, J. D., Burden, R. L., Numerical Methods, 4th ed., Cengage Learning, Boston, Mass., USA, 2012

Paper submitted: October 25, 2015
Paper revised: December 10, 2015
Paper accepted: December 21, 2015